VOL. 18, NO. 18, SEPTEMBER 2023 ISSN 1819-6608
ARPN Journal of Engineering and Applied Sciences

www.arpnjournals.com

AUTOMATIC MEASUREMENT OF CARDIOTHORACIC RATIO IN CHEST X-RAY IMAGES WITH PROGAN-GENERATED DATASET

G. Jagadeeswar Reddy[1], Subba Reddy Borra[2], A. V. Subba Rao[1] and Vaddithandra Vijaya[3]
[1]Newton's Institute of Engineering, Macherla, Andhra Pradesh, India
[2]Information Technology, Malla Reddy Engineering College for Women, Maisammaguda, Hyderabad, India
[3]Computer Science and Engineering (AIML), CMR Institute of Technology, Hyderabad, Telangana, India
E-Mail: jagsuni@yahoo.com

ABSTRACT

Cardiomegaly could be identified using the CTR (Cardiothoracic Ratio), which could be assessed on a chest image or X-ray. It is determined using the link between the size of the heart and chest's transverse dimension. When the ratio exceeds a certain threshold, cardiomegaly is diagnosed. The objective of the study is to offer an approach for calculating the ratio for categorizing cardiomegaly within chest X-ray pictures. The suggested method begins by building heart and lung segmentation models on the basis of U-Net design utilizing publicly accessible datasets containing lung and heart mask ground truth. The segmented lung and heart portion sizes are then used to calculate the ratio. Additionally, chest X-ray images from 3 classes-cardiomegaly, female,and male normal - are created using a novel dataset using PGAN (Progressive Growing of GANs). This dataset is then utilized to evaluate the suggested solution. The suggested approach is also utilized to assess the quality of PGAN-generated chest X-ray pictures. In the trials, lung and heart areas in chest images of X-rays are segmented using trained models and a self-gathered dataset. The computed values of CTR are contrasted with those that were manually assessed by specialists. The average inaccuracy is 3.08 percent. The models are then used to segment areas of the lung and heart for CTR computation on the PGAN dataset. The cardiomegaly is then measured utilizing multiple attempts with varying cut-off threshold values. The proposed approach yields 94.20 percent specificity,88.31% sensitivity, and 94.61% accuracy with the usual cut-off of 0.50. The suggested approach is shown to be resilient across hitherto unexplored datasets for computation of CTR, segmentation, as well as cardiomegaly classification, such as the PGAN dataset. To increase sensitivity, modify the cut-off value to be less than 0.50. The proposed solution is then assessed from a variety of angles, such as lung and heart segmentation, CTR computation, as well as cardiomegaly classification. Tests are also carried out on publicly available datasets, self-collected datasets, as well as ProGAN-reconstructed datasets.

Keywords: the cardiothoracic ratio (CTR), segmentation, progressive growing of GANs (PGAN), cardiomegaly, CTR computation, classification.

Manuscript Received 3 July 2023; Revised 11 November 2023; Published 30 November 2023

1. INTRODUCTION

In clinical practice, the most widely utilized modality for screening for lung and heart disorders is a chest X-ray. Chest X-rays are inexpensive, widely available, and simple to interpret as a 1st line imaging tool. The Cardiothoracic Ratio (CTR), which is obtained from a chest X-ray, is a commonly utilized radiographic indicator for assessing the size of cardiac and providing prognostic data in both congenital as well as acquired heart disorders [1]-[3]. Enlarged CTR is frequently associated with structural cardiac abnormalities as well as cardiac enlargement-related illnesses, and was linked to functional status and poor clinical results [3]. On the other hand, manual CTR computation in ordinary clinical practice is subjective and time-consuming and can cause considerable discrepancies across interpreters.

However, due to the intricacy of anatomical features, reliable interpretation of chest X-rays in CAD (Computer-Aided Diagnostic) systems is particularly difficult. Before further investigation, such as CTR computation, the lung and heart boundaries must be precisely recognized in chest X-rays. Automatic lung and heart field segmentation is a critical and difficult task in computer-aided diagnostic systems. Machine learning has recently become more popular in the medical imaging area, thanks to technological developments in computer science. Deep Learning (DL), one sort of Machine Learning (ML), is becoming the top ML method in the fields of computer vision and medical imaging analysis, and is a developing trend in big data analysing of the medical field [4]-[6]. It was successfully employed in the field of medical imaging, with outstanding results in picture classification, segmentation, and object recognition [7]-[12]. CNNs (Convolutional Neural Networks), a common DLmethodology, automatically learns mid as well as high-level abstractions obtained from fresh data and has proven to be a strong way for problems linked to "medical image processing" [5–6]. CNNs have been used to achieve promising results in the automated segmentation of the liver, tumours, as well as other structures within the brain using MR and CT imaging [9]-[11]. Nevertheless, there was limited use of the interesting DL approach in chest X-rays [13]-[14]. Deep learning can be used to perform automated analysis of chest X-ray pictures. A small data set is used in Reference [15] to

calculate CTR using the DL classic structure U-net, and positive results are obtained.

2. METHOD

The three primary phases in the CTR measurement solution suggested in this study are as follows: ratio calculation, heart segmentation, and lung segmentation.

Figure-1. Illustrations of CTR measurements, where a blue line signifies the largest region of thoracic cavity, an orange line indicates the largest area of the heart, and CTR is the ratio between the lengths of blue and orange lines.

At each layer of the suggested U-Net-based architecture, characteristics are calculated by concatenating characteristics from 3 components: same layer's encoder module, encoder module and decoder module from a below layer. Furthermore, decoder module or expansive section incorporates feature space up-sampling, which employs a 2 3 2 convolution and content with the matching clipped feature space obtained from the contraction part. Therefore, it employs a 3 3 3 convolution layer, followed in ReLu. The last layer employs a 1 3 1 "convolution layer" to obtain the result of segmentation. Figure-2 depicts a sample output.

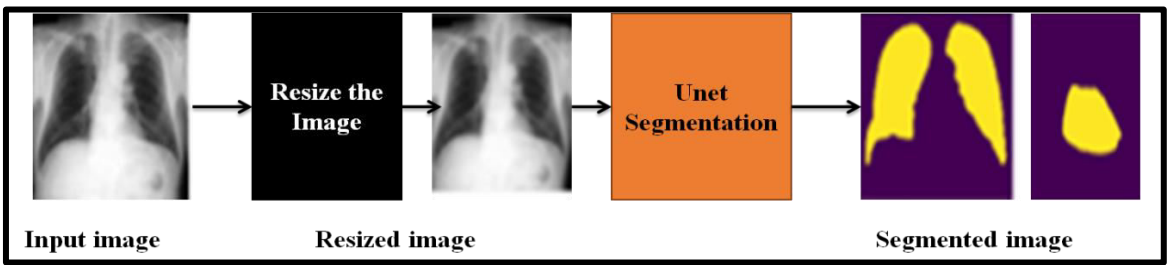

Figure-2. Heart and Lung segmentation sample outputs.

Figure-3. Sample bounding rectangles for the heart and lungs' segmented contours.

As shown in Figure-3, the next stage is to automatically assign bounding rectangles that meet the shapes of segmented lungs and hearts [17, 18]. The thoracic cavity's largest area (L) is then computed by

subtracting the right rightmost position from the left leftmost position. While the heart's broadest area (H) is calculated by determining the fitted bounding rectangle size. CTR is a H L ratio. Cardiomegaly is diagnosed when CTR exceeds a predetermined level. The standard threshold is 0.5. Another major focus of this article is to investigate the use of GAN [19, 20, 21] in producing more samples of testing data with projected ground truth labels. In addition, this study proposes a method for evaluating GAN outputs based on the suggested CTR calculation approach, which would be tested 1st using datasets containing actual ground truth labels. The ProGAN is used in our implementation in this paper. ProGAN suggested a novel training technique for GAN to produce images of unparalleled quality and size. The network's generator and discriminator modules were progressively added as the process of training advanced from a low resolution. A large-scale image might be computed as an output and the fine details may be improved.

3. EXPERIMENTS AND DISCUSSIONS

The three primary sections of our experiments are broken down as follows.

Experiment (a): This experiment has 3 goals: (1) build models of heart and lung segmentation, (2) evaluate segmentation performance, and (3) evaluate CTR calculation performance. The investigation is carried out using publicly available datasets and ground truth masks of lungs as well as hearts inside chest PA x-ray pictures. In trials b and c, the segmentation paradigms created in the test would be utilized to segment hearts and lungs. This is due to the fact that the datasets utilized in trials b and c do not include the ground truth masks of hearts and lungs. As a result, the segmentation models in experiments b and c could not be built.

Experiment (b): This test purpose is to assess the CTR computation on a larger and previously unexplored dataset, a self-collected dataset, using segmentation models developed in experiment (a). This schema could evaluate cross-dataset results when the models are trained on 1 dataset and examined on another. Three human specialists manually measured the ground truth labels of CTR for the self-collected dataset.

Experiment(c): This test is conducted on the produced chest images of PA x-ray with ProGAN. PA x-ray images of 10,000 chests in 3 classes are produced by ProGAN during training: cardiomegaly, female and male normal. The segmentation paradigms learned in test a are then applied to all images to segment hearts and lungs prior to determining CTR. The cut-off criterion on cardiomegaly CTR is adjusted to view the detailed performance.

3.1 Experiment 1

In this experiment, 2 publicly accessible datasets are utilized. For lung segmentation, the first dataset is utilized [22, 23]. It includes appropriate lung mask images for 704 chest X-ray images. Each image has 512 3 512 pixels in resolution. The 2nd dataset, JSRT ("Japanese Society of Radiological Technology") [24], is made up of three sets, comprising 247 chest X-ray images, 247 images of the lung mask, and 247 images of the heart mask [25,26,27]. The size of each chest x-ray image is 2,048 3 2,048 pixels. Nevertheless, the resolution of the lung mask, as well as heart-mask images, is 512 3 512 pixels. Heart and lung segmentation are both done using this second dataset. Each dataset is divided into a 0.6: 0.2: 0.2 ratio of training, validating, and testing sets. The segmentation models are built using the training and validation data. The CTR computation is then assessed using the testing set [28].

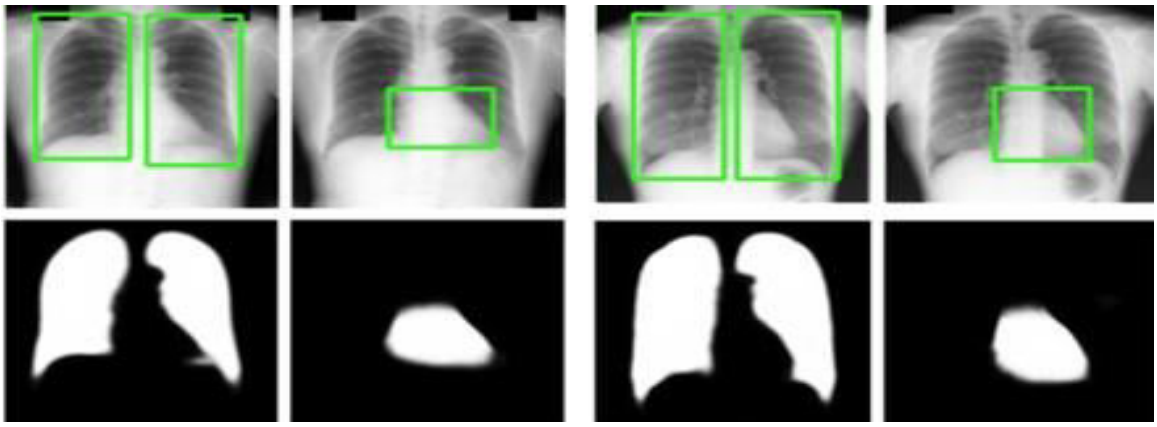

Figure-4. Examples of rectangle fitting on segmented lungs and hearts.

The lung segmentation's training and validating outcomes (namely, pixel-based accuracy) are 0.97 and 0.96, respectively, when the first dataset is used alone. For the training and validation sets, the Dice scores are 0.97 and 0.96, respectively. Moreover, the lung segmentation performance is enhanced by integrating the two datasets. Both the training and validation findings are 0.98, and the Dice scores are likewise 0.98. Additionally, the trained model of heart segmentation is created solely utilizing the second dataset, and it obtains accuracy values

of 0.99 on the training set and 0.98 on the validating set. While the dice scores for the training as well as validating sets are 0.98 and 0.96, respectively.

The segmented lungs, as well as hearts of the two instances, are shown in Figure-4 as examples of rectangle fitting. The region of "thoracic cavity" (L) that is the widest is determined by subtracting the rectangle location that covers the right lung obtained from the rectangle position that covers the left lung. Additionally, rectangle's width enclosing the heart (H) is used to determine its broadest area. The performance of the CTR computation is validated in the following phase of the evaluation. However, neither of these two datasets has a ground truth for CTR. Consequently, to establish the CTR ground truth, the values of CTR are manually assessed with heart and lung mask images.

As stated in Table-1, the performances are quantified in percentage errors. The CTR calculation's error is only 2.98 percent. However, approximately 2.36 percent of the errors were caused by the segmentation of the heart. As seen in Figure-4, heart segmentation is more difficult as compared to lung segmentation because the heart region is placed behind the thoracic vertebrae and has comparable features with surrounding disease traces, like alveolar opacity, consolidation, and ground glass opacity.

Table-1. Performances of the JSRT dataset's CTR calculation.

	"A widest area of thoracic cavity	**A widest area of heart**	**CTR"**
Performance of CTR on JSRT Data set	0.99	2.36	2.98

3.2 Experiment 2

This test is conducted using the dataset of 7,523 chest X-ray images that were self-collected. Every image's resolution is 512 3 512 pixels. The CTR of each image was then manually labelled by three human specialists. The segmentation is used from test 1 because this dataset lacks the ground truth of heart and lung mask pictures. When the models are used to segregate hidden data from our self-collected dataset, they are trained using the datasets from experiment 1. This might be a chance to evaluate the models on the basis of cross-datasets. Table-2 shows the CTR calculation's percentage errors when compared to the manual measurements taken by the 3 specialists.

Table-2. CTR calculation Performances on the self-collected dataset.

	Expert		
Performance of CTR on self-Data set	**1**	**2**	**3**
	3.83	3.30	3.21

The errors are recorded as 3.83 percent, 3.30 percent, and 3.21 percent, respectively compared to the manual dimensions from each specialist. Additionally, the suggested method for the automatic CTR computation might be used as a first line of treatment for the detection of cardiomegaly. Additionally, measurements of the largest areas of the heart and the thoracic cavity could be included in an interactive tool that users might modify further. The approximate acceptable error rate, below which a case will not require extra human editing, is 1.80 percent. In our experiment, 44.27 percent of all instances had a CTR calculation error that is less than 1.80 percent.

3.3 Experiment 3

The dataset of 30,000 chests of PA x-ray images utilized in experiment 3 in this investigation was created using ProGAN. Each of the three classes: normal, female normal, and cardiomegaly-has 10,000 images in total. There are no ground truth lung and heart masks in this dataset. Nevertheless, it is categorized as either having cardiomegaly or not. The three kinds of sample photos produced by ProGAN are displayed below. Additionally, the trained lung and heart segmentation models generated in experiment 1 are used to segment these images. Therefore, the values of CTR are determined accordingly. The values are contrasted against a T-threshold. The cardiomegaly class is assigned if the value is greater than T. If not, it is categorized as being in the normal class. To illustrate the classification accuracy at various threshold levels, the T value ranges from 0.45 to 0.55, as shown in Table-3. According to Table-4, if we stop looking for cardiomegaly at T-threshold 0.50, the accuracy, sensitivity and specificity are 95.61%, 93.31% and 94.45%, respectively. However, a lesser threshold T of 0.45 must be established to achieve a greater sensitivity of 98.76 percent. However, the specificity also decreased to 96.55 percent.

Table-3. Evaluation criteria of the proposed method including Accuracy (%), Sensitivity (%) and Specificity (%).

		Actual		Total	Specificity (%)
		Positive	Negative		
	Positive	TP	FP	TP+FP	TN/(TN+FP)
	Negative	FN	TN	FN+TN	
Total		TP+FN	FP+TN	Accuracy (%): (TP+TN)/(TP+FP+FN+TN)	
Sensitivity (%)		TP/(TP+FN)			

Note: (1) TP: true positive, (2) TN: true negative (3) FP: false positive (4) FN: false negative

Table-4. Performances of CTR calculation on the dataset constructed by ProGAN.

Threshold	Accuracy (%)	Sensitivity (%)	Specificity (%)
0.45	99.85	98.76	96.55
0.46	98.91	96.14	93.61
0.47	98.58	94.79	96.79
0.48	98.84	93.81	97.81
0.49	97.65	90.09	92.66
0.50	95.61	93.31	94.45
0.51	92.89	94.81	96.04
0.52	90.44	89.94	97.16
0.53	89.49	86.02	97.88
0.54	87.03	81.03	96.08
0.55	81.23	79.44	95.26

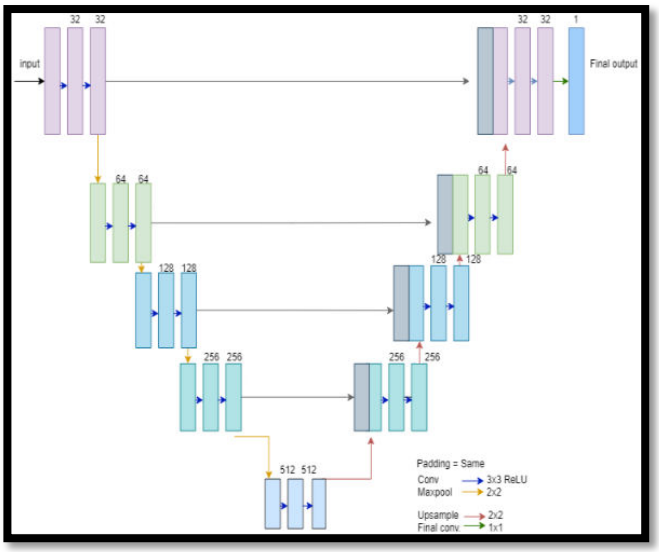

Figure-5. An illustration of U-Net architecture.

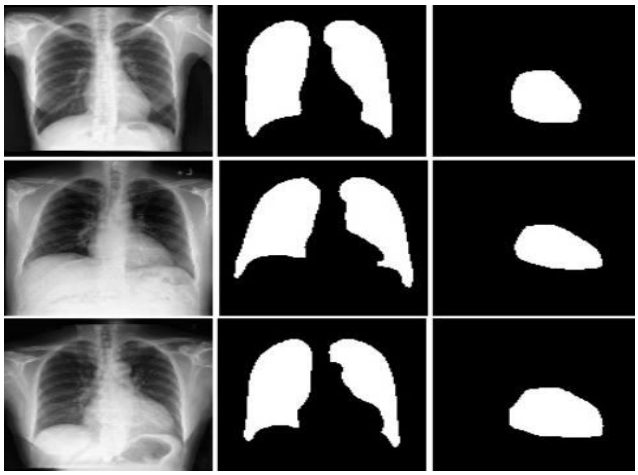

Figure-6. Sample segmented hearts and lungs.

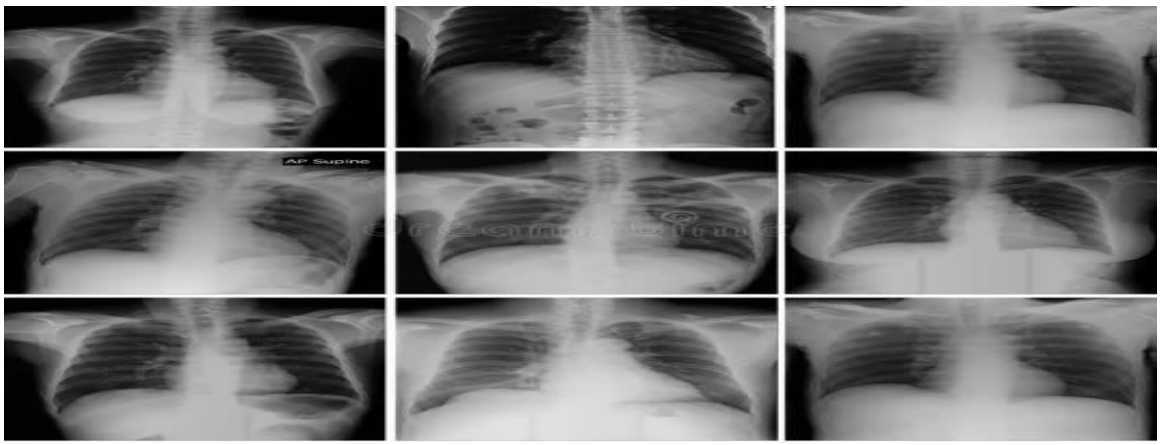

Figure-7. ProGAN-generated examples of the three classes were utilised in Experiment 3. Three samples from the cardiomegaly, male and female normal classes respectively are found in the first, second, and third columns.

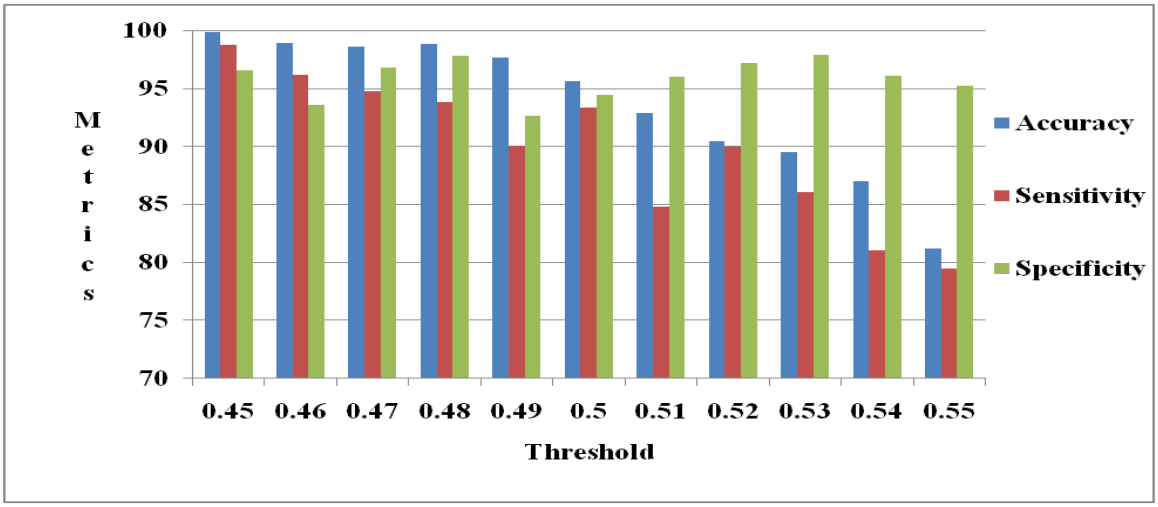

Figure-8. Accuracy, sensitivity, and specificity of various threshold values.

4. CONCLUSIONS

This research created a method that included three processes for lung and heart segmentation, CTR computation, and cardiomegaly classification. Based on the U-Net architecture, the segmentation models were trained and validated using publically available datasets using the mask ground truth. The models were then applied to unexplored datasets, including the self-collected dataset and the new dataset generated by ProGAN, for segmenting portions of the lungs and heart x-ray pictures. The segmented areas were used to generate CTR values, which were subsequently utilised to detect cardiomyopathy by comparing them to the cut-off level. For the CTR calculation on the self-collected dataset, it indicated an average inaccuracy of 3.08%. It also reported an accuracy of 95.61%, sensitivity of 93.31%, and specificity of 94.45% for cardiomegaly classification using the ProGAN dataset. Furthermore, for future work, the built CTR computation programme might be validated in a real-world scenario.

REFERENCES

[1] F. A. Hubbell, S. Greenfield, J. L. Tyler, K. Chetty and F. A. Wyle. 1985. The impact of routine admission chest X-ray films on patient care. New England J. Med. 312: 209-213.

[2] K. Dimopoulos *et al.* 2013. Cardiothoracic ratio from postero-anterior chest radiographs: A simple, reproducible and independent marker of disease severity and outcome in adults with congenital heart disease. Int. J. Car-diol. 166: 53-457.

[3] G. Chartrand *et al.* 2017. Deep learning: A primer for radiologists. Radio-graphics. 37(7): 2113-2131.

[4] T. Kooi *et al. 2017.* Large scale deep learning for computer aid detection of mammographic lesions. Med. Image Anal. 35: 303-312.

[5] S. Wang *et al.* 2017. Central focused convolutional neural networks: Develop-in a data-driven model for lung nodule segmentation. Med. Image Anal. 40: 172-183.

[6] M. Drozdzal *et al.* 2018. Learning normalized inputs for iterative estimation in medical image segmentation. Med. Image Anal. 44: 1-13.

[7] P. Moeskops, M. A. Viergever, A. M. Mendrik, L. S. de Vries, M. J. N. L. Benders and I. Išgum. 2016. Automatic segmentation of MR brain images with a convolutional neural network. IEEE Trans. Med. Imag. 35(5): 1252-1261.

[8] S. Pereira, A. Pinto, V. Alves and C. A. Silva. 2016. Brain tumor segmentation using convolutional neural networks in MRI images. IEEE Trans. Med. Imag. 35(5): 1240-1251.

[9] M. Anthimopoulos, S. Christodoulidis, L. Ebner, A. Christe and S. Mougiakakou. 2016. Lung pattern classification for interstitial lung diseases using a deep convolutional neural network. IEEE Trans. Med. Imag. 35(5): 1207-1216.

[10] M. Cicero *et al.* 2017. Training and validating a deep convolutional neural network for computer-aided detection and classification of abnormalities on frontal chest radiographs. *Invest. Radiol.* 52(5): 281-287.

[11] O. Ronneberger, P. Fischer and T. Brox. 2015. U-Net: Convolutional networks for biomedical image segmentation. in Medical Image Computing and Computer-Assisted Intervention-MICCAI. Cham, Switzerland: Springer. pp. 234-241.

[12] S. Honari, J. Yosinski, P. Vincent and C. Pal. 2016. Recombinator networks: Learning coarse-to-fine feature aggregation. in Proc. IEEE Comput. Vis. Pattern Recognit. pp. 5743-5752.

[13] X. Glorot and Y. Bengio. 2010. Understanding the difficulty of training deep feed forward neural networks. J. Mach. Learn. Res. 9: 249-256.

[14] D. E. Rumelhart, G. E. Hinton and R. J. Williams. 1988. Learning representations by back-propagating errors. in Neurocomputing: Foundations of Research, Cambridge, MA, USA: MIT Press. pp. 533-536.

[15] P. Krähenbühl and V. Koltun. 2012. Efficient inference in fully connected CRFs with Gaussian edge potentials,'' in Proc. Adv. Neural Inf. Process. Syst. pp. 109-117.

[16] Z. Li, Z. Hou, C. Chen, Z. Hao, Y. An, S. Liang and B. Lu. 2019. Automatic cardiothoracic ratio calculation with deep learning. IEEE Access. 7: 37749-37756.

[17] I. M. Baltruschat, H. Nickisch, M. Grass, T. Knopp and A. Saalbach. 2019. Comparison of deep learning approaches for multi-label chest X-ray classification. Sci. Rep. 9(1): 1-10.

[18] N. Sezaki and K. Ukena. 1974. Automatic computation of the cardiothoracic ratio with application to mass screening. IEEE Trans. Biomed. Eng. BE-20(4): 248-259.

[19] M. Cicero, A. Bilbily, E. Colak, T. Dowdell, B. Gray, K. Perampaladas and J. Barfett. 2017. Training and validating a deep convolutional neural network for computer-aided detection and classification of abnormalities on frontal chest radiographs. Invest. Radiol. 52(5): 281-287.

[20] Z. Li, Z. Hou, Z. Hao, Y. An, S. Liang, B. Lu and C. Chen. 2019. Automatic cardiothoracic ratio calculation with deep learning. IEEE Access. 7: 37749-37756.

[21] K. Truszkiewicz, R. Poreba and P. Gac. 2021. Radiological cardiothoracic ratio in evidence-based medicine. J. Clin. Med. 10: 1-9.

[22] W. Chaisangmongkon, I. Chamveha, T. Promwiset, P. Saiviroonporn and T. Tongdee. 2021. External validation of deep learning algorithms for cardiothoracic ratio measurement. IEEE Access. 9: 110287-110298.

[23] M.Drozdzal, E. Vorontsov, G. Chartrand, S. Kadoury and C. Pal. 2016. The Importance of Skip Connections in Biomedical Image Segmentation (Lecture Notesin Computer Science). Cham, Switzerland: Springer.

[24] S. Kiranyaz, O. Avci, O. Abdeljaber, T. Ince, M. Gabbouj and J. Daniel Inman. 2021. 1D convolutional neural networks and applications: A survey. Mech. Syst. Signal Process. 151(Art.no.107398).

[25] Q. Que, Z. Tang, R. Wang, Z. Zeng, J. Wang, M. Chua, T.S. Gee, X. Yang and B. Veeravalli. 2018.

Cardio XNet: Automated detection for cardiomegaly based on deep learning. in Proc. 40th Annu. Int. Conf. IEEE Eng. Med. Biol. Soc. (EMBC). pp. 612-615.

[26] J. Y. Lu, P. -Y. Lee and C.-C. Huang. 2022. Improving image equality for single-angle plane wave ultrasound imaging with convolutional neural network beam for me. IEEE Trans. Ultrason., Ferroelectr. Freq. Control. 69(4): 1326-1336.

[27] O. A. Centurión, E. K. Scavenius, M. L. Miño and R. O. Sequeira. 2017. Evaluating cardiomegaly by radiological cardiothoracic ratio as compared to conventional echocardiography. J. Cardiol. Current Res. 9(2): 1-3.